Nimardeep Kaur, Rupinder Kaur and N. S. Saini*

Ion-Acoustic Cnoidal Waves with the Density Effect of Spin-up and Spin-down Degenerate Electrons in a Dense Astrophysical Plasma

https://doi.org/10.1515/zna-2019-0140 Received April 26, 2019; accepted November 4, 2019; previously published online December 7, 2019

Abstract: An investigation of nonlinear ion acoustic (IA) cnoidal waves in a magnetised quantum plasma is presented by using spin evolution quantum hydrodynamics model, in which inertial classical ions and degenerate inertialess electrons with both spin-up and spin-down states taken as separate species are considered. The Korteweg-de Vries equation is derived using the reductive perturbation method. Further, using the Sagdeev pseudopotential approach, the solution for IA cnoidal waves is derived with suitable boundary conditions. There is the formation of only positive potential cnoidal, and in the limiting case, positive solitary waves are observed. The effects of density polarisation and other plasma parameters on the characteristic features of cnoidal and solitary waves have been analysed numerically. It is seen that the spin density polarisation significantly affects the characteristics of cnoidal structures as we move from strongly spin-polarised ($\mu = 1$) to a zero spin-polarisation case $(\mu = 0)$. The results obtained in the present investigation may be useful in comprehending various nonlinear excitations in dense astrophysical regions, such as white dwarfs, neutron stars, and so on.

Keywords: Cnoidal Waves; Ion Acoustic; Spin-up and Spin-down Degenerate Electrons.

1 Introduction

In recent years, dense quantum plasmas have emerged as an active field of research due to their great relevance in different areas of practical importance, e.g. nanoscale

*Corresponding author: N. S. Saini, Department of Physics, Guru Nanak Dev University, Amritsar 143005, India, E-mail: nssaini@yahoo.com

Nimardeep Kaur and Rupinder Kaur: Department of Physics, Guru Nanak Dev University, Amritsar 143005, India, E-mail: nimarphy@gmail.com (N. Kaur); rupinderkaur.rk568@gmail.com (R. Kaur) electromechanical systems [1, 2], laser interactions with atomic systems [3], and in dense astrophysical systems [4], such as neutron stars, white dwarfs, and so on. Due to the high number density and low particle temperature of particles, quantum plasmas are distinguished significantly from the classical plasmas, where the density of particles is relatively low and possesses high plasma temperature. To investigate the various astrophysical phenomena in interstellar compact objects, dense quantum plasmas would be helpful in establishing a suitable frame. The density of the interiors of the interstellar objects is significantly high such that the nonthermal pressure is provided by the degenerate fermion/electron pressure, as well as interaction of particles.

Mathematically, Chandrashekhar [5–7] deduced the equation of state in such compact interstellar objects for the degenerate electrons with $P_e \sim n_e^{\frac{3}{2}}$ for the nonrelativistic case and $P_e \sim n_e^{\frac{4}{3}}$ for the ultrarelativistic case, where P_e and n_e are the pressure and number density of degenerate electrons. In highly compressed plasma species, the uncertainty in momenta is infinitely large, which implies that the degenerate plasma species must move very fast (despite that they are extremely cold), giving rise to a very high pressure, called as "degenerate pressure." The degenerate pressure depends only on the number density of electrons and not on their temperature. In the quantum hydrodynamic (QHD) model, which is considered as the quantum counterpart of the classical fluid model [8], the inclusion of the Fermi pressure and the Bohm potential term modifies the momentum equation of the charged particles [9]. The quantum ion acoustic (IA) waves and the role of quantum diffraction effects have been studied by Haas et al. [10] using the QHD model. It has also been found that the system supports the travelling waves with periodic patterns in the fully nonlinear regime. Haas [11] devised an ideal quantum magnetohydrodynamic (QMHD) model with the incorporation of the quantum diffraction effects with relevance to the dense astrophysical objects such as interiors of white dwarfs. Using the QHD and QMHD models, various nonlinear electrostatic and electromagnetic waves have been studied in quantum plasmas.

The spin effects are considered as one of the most important properties of quantum plasmas due to great significance of highly magnetised quantum plasmas in the atmospheres of neutron stars [12, 13]. Marklund and Brodin [14, 15] extended the QMHD model and proposed the spin- $\frac{1}{2}$ QMHD model for hydrodynamic waves. They found that the spin effects can significantly alter the characteristics of low-frequency electromagnetic modes. The dynamics of fast and slow magnetosonic waves has been studied by Mushtag and Vladimirov [16] in two-dimensional spin- $\frac{1}{2}$ quantum plasmas using QMHD model. The linear dispersion relation for both slow and fast quantum magnetosonic waves has been discussed in detail. Andreev [17] considered the propagation of waves with degenerate electrons in the magnetised plasmas and derived the QHD equations for spin- $\frac{1}{2}$ particles. The author examined the evolution of electrons and contribution of magnetic field in the Langmuir wave dispersion via the different occupation of spin-up and spin-down states. The existence of spin-electron-positron acoustic spin-electron acoustic, and positron acoustic solitons in degenerate electron-positron-ion (e - p - i) plasmas were demonstrated by Iqbal and Andreev [18]. The influence of the spin polarisation on the properties of three kinds of solitons was also analysed. It has been reported that there exist different types of spin-up and spin-down electrons in metal in the absence of an external magnetic field, which yields magnetic moment of metal as a whole equal to zero [19]. But in the presence of an external uniform magnetic field, there are more electrons with spin-up aligned along the direction of magnetic field than that of spin-down electrons. Owing to the presence of spin-up and spin-down electrons in a degenerate quantum plasma, some investigations focusing on the study of solitary and shock waves have been reported. Ahmad et al. [20] investigated the lowfrequency electrostatic waves in plasmas having inertialess degenerate electrons by employing the separated spin evolution QHD model. The pulse stability analysis was carried out, and it was also found that spin polarisation significantly affects the amplitude and width of the solitary waves. Hussain and Mahmood [21] investigated the propagation characteristics of IA shock waves in a dense magnetised plasma with relative density effects of spinup and spin-down degenerate electrons. The Korteweg-de Vries Burgers equation was solved numerically to analyse the influence of the spin density polarisation ratio on the propagation characteristics of shock waves.

The study of cnoidal waves has become one of the important areas of research because of their wide range of applications in nonlinear transport processes in plasmas [22], ionosphere plasmas [23], single-mode drift wave spectra [24], and so on. A variety of investigations have been reported by numerous researchers [25-28] to study the characteristics of cnoidal waves in different plasma regimes. Kaladze et al. [29] deduced Korteweg-de Vries (KdV) equation by employing the reductive perturbation method and investigated electrostatic acoustic nonlinear periodic waves in unmagnetised pair-ion plasmas that constitute the same mass ion species with different temperatures. El-Shamy [25] investigated the propagation characteristics of IA cnoidal waves in a dense relativistic degenerate magnetoplasma consisting of relativistic degenerate electrons and nondegenerate cold ions. The various solutions of nonlinear cnoidal and solitary waves were presented numerically. Ur-Rehman et al. [26] derived the KdV equation in a magnetised e - i plasma with cold ions and warm electrons. The impact of various plasma parameters on the characteristics of compressive magnetoacoustic cnoidal waves was studied. The propagation properties of dust acoustic cnoidal waves in an unmagnetised ion beam dusty plasma were investigated by Kaur et al. [27]. Using reductive perturbation technique, the KdV equation was derived, and the solution of nonlinear cnoidal waves was determined by applying the appropriate boundary conditions. The characteristic features of magnetosonic cnoidal and solitary waves were investigated in a magnetised electron-ion-dust (e-i-d) plasma by Kaur et al. [28]. It was found that there exist only positive potential magnetosonic cnoidal and solitary waves in the limit of high β plasma.

Earlier investigations were focussed on the study of solitary and shock waves in a degenerate quantum plasma with the effects of the spin-up and spin-down of the electrons. To the best of our knowledge, the study of IA cnoidal waves with the effects of both spin-up and spindown of degenerate electrons in a magnetised quantum plasma has not been reported yet. Our aim in the present investigation is to numerically analyse the effect of spin polarisation density and other physical parameters on the propagation characteristics of IA cnoidal waves in dense astrophysical plasma with implication to the region of white dwarfs. The layout of the manuscript is as follows: In Section 2, the basic fluid equations are introduced. In Section 3, the derivation of the nonlinear KdV equation by using reductive perturbation method is presented. The cnoidal wave solution of KdV equation is given in Section 4. In Section 5, the numerical analysis for IA cnoidal waves and in the limiting case solitary waves has been presented. Conclusions are highlighted in Section 6.

Basic Fluid Equations

We consider a magnetised quantum plasma in which a uniform magnetic field is applied along the positive zdirection, $B = B_0 \hat{z}$. The separated spin evolution QHD model has been utilised by considering both the spin-up $(n_{e\uparrow})$ and spin-down $(n_{e\downarrow})$ states for degenerate electrons and inertial nondegenerate ions. Here, we assume that wave propagates in three dimensions, i.e. $\nabla = \partial_x, \partial_y, \partial_z$. Nondegenerate ions are taken due to their heavy mass as compared to the mass of electrons. The separate evolution of spin-up and spin-down electrons helps to discover the new longitudinal waves, which depend on parallel and perpendicular propagation to an external magnetic field. Their existence is related to the different population of spin-up and spin-down electrons in equilibrium plasmas [17]. The continuity and momentum equations for ions are given as

$$\frac{\partial n_i}{\partial t} + \nabla \cdot (n_i \mathbf{u}_i) = 0, \tag{1}$$

$$\left(\frac{\partial}{\partial t} + \mathbf{u}_i \cdot \nabla\right) \mathbf{u}_i = \frac{e}{m_i} \mathbf{E} + \frac{eB_0}{m_i c} \mathbf{u}_i \times \hat{z}. \tag{2}$$

Electrons are inertialess, and the momentum equations of electrons with spin-up $(n_{e\uparrow})$ and spin-down $(n_{e\downarrow})$ states are given as

$$0 = -e n_{e\uparrow(\downarrow)} \left(\mathbf{E} + \frac{B_0}{c} \mathbf{u}_{e\uparrow(\downarrow)} \right) - \nabla P_{e\uparrow(\downarrow)}$$

$$+ \frac{\hbar^2}{2m_e} n_{e\uparrow(\downarrow)} \nabla \left(\frac{\nabla^2 \sqrt{n_{e\uparrow(\downarrow)}}}{\sqrt{n_{e\uparrow(\downarrow)}}} \right). \tag{3}$$

The Poisson's equation is given as

$$\nabla \cdot \mathbf{E} = 4\pi e (n_i - n_{e|} + n_{e\uparrow}). \tag{4}$$

The Fermi pressure of degenerate electrons with spinup $(n_{e\uparrow})$ and spin-down $(n_{e\downarrow})$ is $P_{e\uparrow}=rac{K_BT_{F_{e\uparrow}}n_{e\uparrow}^{2}}{5n_{c\uparrow}^{2}}$ and $P_{e\downarrow} = rac{K_B T_{F_{e\uparrow}} n_{e\uparrow}^{rac{5}{2}}}{5 n_{0\downarrow}^{rac{2}{3}}}. \ T_{F_{e\uparrow}} = rac{6 \pi^2 n_{0\uparrow}^{rac{2}{3}} \hbar^2}{2 K_B m_e} \ ext{and} \ T_{F_{e\downarrow}} = rac{6 \pi^2 n_{0\downarrow}^{rac{2}{3}} \hbar^2}{2 K_B m_e} \ ext{are}$ the Fermi temperatures for spin-up $(n_{e\uparrow})$ and spin-down $(n_{e|})$ electrons, respectively; K_B is the Boltzmann constant. In this model, ion temperature is ignored as compared to electron temperature.

In component form, the normalised continuity and momentum equations for ions are written as

$$\frac{\partial n_i}{\partial t} + \frac{\partial}{\partial x}(n_i u_{ix}) + \frac{\partial}{\partial y}(n_i u_{iy}) + \frac{\partial}{\partial z}(n_i u_{iz}) = 0, \quad (5)$$

$$\frac{\partial}{\partial t}u_{ix}+Du_{ix}=-\frac{\partial\phi}{\partial x}+\Omega u_{iy}, \qquad (6)$$

$$\frac{\partial}{\partial t}u_{iy} + Du_{iy} = -\frac{\partial \phi}{\partial y} - \Omega u_{ix}, \tag{7}$$

$$\frac{\partial}{\partial t}u_{iz} + Du_{iz} = -\frac{\partial \phi}{\partial z}.$$
 (8)

The component forms of the normalised momentum equations for spin-up and spin-down electrons are written

$$0 = \frac{\partial \phi}{\partial x} - \Omega u_{ey\uparrow(\downarrow)} - \frac{(2\mu_{\uparrow(\downarrow)})^{\frac{2}{3}}}{3} n_{e\uparrow(\downarrow)}^{-\frac{1}{3}} \frac{\partial n_{e\uparrow(\downarrow)}}{\partial x} + \frac{H^{2}}{2} \frac{\partial}{\partial x} \left(\frac{\nabla^{2} \sqrt{n_{e\uparrow(\downarrow)}}}{\sqrt{n_{e\uparrow(\downarrow)}}} \right), \tag{9}$$

$$0 = \frac{\partial \phi}{\partial y} - \Omega u_{ex\uparrow(\downarrow)} - \frac{(2\mu_{\uparrow(\downarrow)})^{\frac{2}{3}}}{3} n_{e\uparrow(\downarrow)}^{-\frac{1}{3}} \frac{\partial n_{e\uparrow(\downarrow)}}{\partial y} + \frac{H^2}{2} \frac{\partial}{\partial y} \left(\frac{\nabla^2 \sqrt{n_{e\uparrow(\downarrow)}}}{\sqrt{n_{e\uparrow(\downarrow)}}} \right), \tag{10}$$

$$0 = \frac{\partial \phi}{\partial z} - \frac{(2\mu_{\uparrow(\downarrow)})^{\frac{2}{3}}}{3} n_{e\uparrow(\downarrow)}^{-\frac{1}{3}} \frac{\partial n_{e\uparrow(\downarrow)}}{\partial z} + \frac{H^2}{2} \frac{\partial}{\partial z} \left(\frac{\nabla^2 \sqrt{n_{e\uparrow(\downarrow)}}}{\sqrt{n_{e\uparrow(\downarrow)}}} \right). \tag{11}$$

The normalised Poisson's equation is

$$\frac{\partial^{2}\phi}{\partial x^{2}} + \frac{\partial^{2}\phi}{\partial y^{2}} + \frac{\partial^{2}\phi}{\partial z^{2}} = \mu_{\uparrow}n_{e\uparrow} + \mu_{\downarrow}n_{e\downarrow} - n_{i}$$
 (12)

where $\mu_{\uparrow}=rac{n_{0\uparrow}}{n_{i0}}$ and $\mu_{\downarrow}=rac{n_{0\downarrow}}{n_{i0}}$. The charge neutrality condition yields $n_{e0\uparrow}+n_{e0\downarrow}=n_{i0}$. The density polarisation ratio is given as

$$\mu = \frac{n_{e0\uparrow} - n_{e0\downarrow}}{n_{e0\uparrow} + n_{e0\downarrow}},\tag{13}$$

It is seen that μ can be positive, zero, or negative. $0 < \mu \ (\mu < 0)$ corresponds to plasmas where the number density of spin-up electrons is higher (lower) than that of the spin-down electrons. When two electron species have equal number densities, then $\mu = 0$. From (13), the negative value of μ has no physical significance because in the presence of an external uniform magnetic field there are more electrons with spin-up aligned along the direction of the magnetic field than that of spin-down electrons [19]. For the case $\mu = 1$ (i.e. electrons have only one state of spin), one can simply recover the case of e-i plasmas. Therefore, $\mu_{\uparrow}=\frac{1+\mu}{2}$ and $\mu_{\downarrow}=\frac{1-\mu}{2}$. $D=\mathbf{u}\cdot\nabla$ is the convective derivative, $\Omega=\frac{\omega_{ci}}{\omega_{pi}}$, where Ω is the ion-cyclotron frequency, $\omega_{ci}=\frac{eB_0}{m_ic}$ is normalised by ion plasma frequency $\omega_{pi}=\sqrt{\frac{4\pi n_{i0}e^2}{m_i}}$, and $H=\frac{\hbar\omega_{pi}}{\sqrt{m_im_ec_s^2}}$ is the quantum parameter. The fluid velocities (u_{ix},u_{iy},u_{iz}) are normalised by the quantum IA speed $c_s=\sqrt{\frac{2k_BT_F}{m_i}}$; the number densities $n_i,n_{e\uparrow},n_{e\downarrow}$ are normalised by their respective equilibrium number densities and electrostatic potential ϕ by $\frac{2k_BT_F}{e}$. The space coordinates are normalised by $\lambda_i=\frac{c_s}{\omega_{pi}}$ and time by the inverse of the ion-plasma frequency (ω_{ni}^{-1}) .

3 Derivation of the KdV Equation

We have employed the reductive perturbation method to derive the KdV equation for the study of cnoidal waves in a magnetised dense astrophysical quantum plasma. The stretching coordinates are given as

$$\xi = \varepsilon^{\frac{1}{2}}(k_x x + k_y y + k_z z - v_{ph}t), \tau = \varepsilon^{\frac{3}{2}}t.$$
 (14)

where k_x , k_y , and k_z are the direction cosines such that $k_x^2 + k_y^2 + k_z^2 = 1$, and v_{ph} is the phase velocity of the waves. Here, ε is a small expansion parameter. The perturbed quantities n_i , u_{ix} , u_{iy} , u_{iz} , and ϕ are expanded in terms of smallness parameter ε in the following form:

$$n_{i,e} = 1 + \varepsilon n_{i,e}^{(1)} + \varepsilon^{2} n_{i,e}^{(2)} + \dots$$

$$u_{(i,e)x} = \varepsilon^{\frac{3}{2}} u_{(i,e)x}^{(1)} + \varepsilon^{2} u_{(i,e)x}^{(2)} + \dots$$

$$u_{(i,e)y} = \varepsilon^{\frac{3}{2}} u_{(i,e)y}^{(1)} + \varepsilon^{2} u_{(i,e)y}^{(2)} + \dots$$

$$u_{(i,e)z} = \varepsilon u_{(i,e)z}^{(1)} + \varepsilon^{2} u_{(i,e)z}^{(2)} + \dots$$

$$\phi = \varepsilon \phi^{(1)} + \varepsilon^{2} \phi^{(2)} + \dots$$
(15)

Using (14) and (15) in (5)–(12) and collecting the terms in the lowest order of ε , we get the following first-order evolution equations.

From ion continuity equation:

$$-\nu_{ph}\frac{\partial n_i^{(1)}}{\partial \xi} + k_z \frac{\partial u_{iz}^{(1)}}{\partial \xi} = 0, \tag{16}$$

From the z-component of the ion momentum equation:

$$k_z \frac{\partial \phi^{(1)}}{\partial \xi} = \nu_{ph} \frac{\partial u_{iz}^{(1)}}{\partial \xi},\tag{17}$$

From the *z*-component of electron momentum equation having the spin-up state:

$$\frac{\partial \phi^{(1)}}{\partial \xi} = \frac{(2\mu_{\uparrow})^{\frac{2}{3}}}{3} n_{e\uparrow}^{\frac{1}{3}} \frac{\partial n_{e\uparrow}^{(1)}}{\partial \xi},\tag{18}$$

From the *z*-component of the electron momentum equation having the spin-down state:

$$\frac{\partial \phi^{(1)}}{\partial \xi} = \frac{(2\mu_{\downarrow})^{\frac{2}{3}}}{3} n_{e\downarrow}^{\frac{1}{3}} \frac{\partial n_{e\downarrow}^{(1)}}{\partial \xi}.$$
 (19)

From Poisson's equation:

$$\mu_{\uparrow} n_{e\uparrow}^{(1)} + \mu_{\downarrow} n_{e\downarrow}^{(1)} = n_i^{(1)},$$
 (20)

On solving (16)–(19), the phase velocity for IA cnoidal waves having both spin-up and spin-down states of degenerate electrons is obtained as

$$\nu_{ph} = k_z \sqrt{\frac{2^{\frac{2}{3}}}{3(\mu_{\uparrow}^{\frac{1}{3}} + \mu_{\downarrow}^{\frac{1}{3}})}}$$
 (21)

On integrating (16)–(19) and applying some algebraic manipulations, we get the following relations:

$$n_i^{(1)} = \frac{k_z^2}{V_{nh}^2} \phi^{(1)} + C_1(\tau),$$
 (22)

$$u_{iz}^{(1)} = \frac{k_z}{v_{ph}} \phi^{(1)} + C_2(\tau),$$
 (23)

$$n_{e\uparrow}^{(1)} = \frac{3}{(2\mu_{\uparrow})^{\frac{2}{3}}} \phi^{(1)} + C_3(\tau),$$
 (24)

$$n_{e\downarrow}^{(1)} = \frac{3}{(2\mu_1)^{\frac{2}{3}}} \phi^{(1)} + C_4(\tau).$$
 (25)

where $C_1(\tau)$, $C_2(\tau)$, $C_3(\tau)$, and $C_4(\tau)$ are the integration constants, which may depend on τ but independent of ξ .

Collecting the next higher-order terms of ε in the ion continuity equation, we have

$$-\nu_{ph}\frac{\partial n_{i}^{(2)}}{\partial \xi} + \frac{\partial n_{i}^{(1)}}{\partial \tau} + k_{x}\frac{\partial u_{ix}^{(2)}}{\partial \xi} + k_{y}\frac{\partial u_{iy}^{(2)}}{\partial \xi} + k_{z}\frac{\partial u_{iz}^{(2)}}{\partial \xi} + k_{z}\frac{\partial}{\partial \xi}(n_{i}^{(1)}u_{iz}^{(1)}) = 0.$$
 (26)

Collecting the next higher-order terms of the z-component of the momentum equation of ions, we have

$$-v_{ph}\frac{\partial u_{iz}^{(2)}}{\partial \xi} + \frac{\partial u_{iz}^{(1)}}{\partial \tau} + k_z u_{iz}^{(1)} \frac{\partial u_{iz}^{(1)}}{\partial \xi} = -k_z \frac{\partial \phi^{(2)}}{\partial \xi}.$$
 (27)

The next higher-order terms of the z-component of the momentum equations of electrons having spin-up and spin-down states give the following equations:

$$k_{z} \frac{\partial \phi^{(2)}}{\partial \xi} - \frac{(2\mu_{\uparrow(\downarrow)})^{\frac{2}{3}}}{3} k_{z} \frac{\partial n_{e\uparrow(\downarrow)}^{(2)}}{\partial \xi} + \frac{H^{2}}{4} k_{z}^{3} \frac{\partial^{3} n_{e\uparrow(\downarrow)}^{(1)}}{\partial \xi^{3}}$$
$$+ \frac{(2\mu_{\uparrow(\downarrow)})^{\frac{2}{3}}}{9} k_{z} n_{e\uparrow(\downarrow)}^{(1)} \frac{\partial n_{e\uparrow(\downarrow)}^{(1)}}{\partial \xi} = 0. \tag{28}$$

The next higher-order terms of the Poisson's equation

$$\frac{\partial^2 \phi^{(1)}}{\partial \xi^2} = \mu_{\uparrow} n_{i\uparrow}^{(2)} + \mu_{\downarrow} n_{i\downarrow}^{(2)} - n_i^{(2)}. \tag{29}$$

On simplifying (26)–(29) by eliminating the second-order quantities and making use of the boundary conditions $\frac{\partial C_1(\tau)}{\partial \tau} = \frac{\partial C_2(\tau)}{\partial \tau} = \frac{\partial C_3(\tau)}{\partial \tau} = \frac{\partial C_4(\tau)}{\partial \tau} = 0$, we obtain the following form of the KdV equation:

$$\frac{\partial \phi^{(1)}}{\partial \tau} + A \phi^{(1)} \frac{\partial \phi^{(1)}}{\partial \xi} + B \frac{\partial^3 \phi^{(1)}}{\partial \xi^3} + C \frac{\partial \phi^{(1)}}{\partial \xi} = 0 \quad (30)$$

where the nonlinear coefficient *A*, dispersion coefficient *B*, and the coefficient *C* are given as

$$A = \frac{3k_z}{2} \left(1 - \frac{1}{2^{\frac{4}{3}} (\mu_{\uparrow}^{\frac{1}{3}} + \mu_{\downarrow}^{\frac{1}{3}})} \right),$$

$$B = \frac{v_{ph}^3}{2k_z^2} \left(1 + \frac{(1 - k_z^2)}{\Omega^2} - \frac{9H^2}{2^{\frac{4}{3}} (\mu_{\uparrow}^{\frac{1}{3}} + \mu_{\downarrow}^{\frac{1}{3}})} \right),$$

$$C = \frac{v_{ph}^3}{2k_z^2} \left(\frac{k_z^4}{v_{ph}^4} C_2 - \frac{\mu_{\uparrow}^{\frac{1}{3}}}{2^{\frac{2}{3}}} C_3 - \frac{\mu_{\downarrow}^{\frac{1}{3}}}{2^{\frac{2}{3}}} C_4 \right). \tag{31}$$

In the limiting case, when coefficient C vanishes in (38) of [20] and in (29) of [21], one can get the KdV equation, which agrees with (30) (for C=0) in the present investigation.

4 Cnoidal Wave Solution of the KdV Equation

The stationary solution of (30) is obtained by using the transformation $\eta = \xi - U_1 \tau$; here, U_1 is velocity of nonlinear cnoidal waves. By changing (30) into η coordinate and applying some algebraic simplifications, the energy balance equation is obtained as

$$\frac{1}{2} \left(\frac{\partial \phi}{\partial \eta} \right)^2 + V(\phi) = 0, \tag{32}$$

where $V(\phi)$ is the Sagdeev potential, which is given as

$$V(\phi) = \frac{A}{6B}\phi^3 - \frac{U}{2B}\phi^2 + \rho_0\phi - \frac{1}{2}E_0^2$$
 (33)

 ho_0 and E_0 are the integration constants representing the charge density and the electric field, respectively. $U=U_1-C$ and $E_0^2/2$ are the total energy of oscillations. By using the initial boundary conditions $\phi(0)=\phi_0$ and $\frac{\partial \phi(0)}{\partial \eta}=0$, the expression for electric field E_0 is obtained as

$$E_0^2 = \frac{A}{3B}\phi_0^3 - \frac{U}{B}\phi_0^2 + 2\rho_0\phi_0 \tag{34}$$

Substituting (33) and (34) in (32) and after some mathematical calculations, we obtain

$$\left(\frac{\partial \phi}{\partial \eta}\right)^2 = \frac{A}{3B}(\phi_0 - \phi)(\phi - \phi_1)(\phi - \phi_2) \tag{35}$$

where ϕ_1 and ϕ_2 are the real roots of Sagdeev potential, which are given as

$$\phi_{1,2} = \frac{3}{2} \left[\frac{U}{A} - \frac{\phi_0}{3} \pm \sqrt{\frac{1}{2} (\beta_1 - \phi_0)(\phi_0 - \beta_2)} \right],$$
 (36)

and

$$\beta_{1,2} = \frac{U}{A} \pm 2\sqrt{\frac{U^2}{A^2} - 2\rho_0 \frac{B}{A}},\tag{37}$$

To find the periodic wave solution of IA waves, the inequalities $\beta_2 \leq \phi_0 \leq \beta_1$ or $\beta_1 \leq \phi_0 \leq \beta_2$ must be satisfied. The periodic wave solution (31) of [30] is given as

$$\phi(\eta) = \phi_1 + \phi_{cn} c n^2(G\eta, m) \tag{38}$$

where cn is the Jacobian elliptic function, and the parameters m and G are defined as $m^2 = \frac{(\phi_0 - \phi_1)}{(\phi_0 - \phi_2)}$ and $G = \sqrt{\frac{A}{12B}(\phi_0 - \phi_2)}$, where m^2 is varied as $0 \le m \le 1$. The amplitude and the wavelength of the cnoidal wave are defined as $\phi_{cn} = (\phi_0 - \phi_1)$ and $\lambda = 4\sqrt{\frac{3B}{A(\phi_0 - \phi_1)}}K(m)$, where K(m) is the complete elliptic integral of the first kind.

For the case, $m \to 1$ $(E_0 = \rho_0 = 0)$ at $\phi_1 = \phi_2 = 0$, $\phi_{cn} = \phi_0 = \frac{3U}{A} = \phi_m$, $G = \left(\frac{A\phi_0}{12B}\right)^{1/2} = \left(\frac{U}{4B}\right)^{1/2} = \frac{1}{w}$, and cn $\delta = \mathrm{sech}$ δ , the cnoidal wave solution reduces to the following solitary wave solution [31]

$$\phi(\eta) = \phi_m \operatorname{sech}^2\left(\frac{\eta}{w}\right),\tag{39}$$

where $\phi_m = \frac{3U}{A}$ and $w = \sqrt{\frac{4B}{U}}$ are the peak amplitude and the width of the IA solitary waves, respectively.

It is evident from (21), (31), and (39) that the propagation characteristics of IA cnoidal and solitary waves show the dependence on various plasma parameters such as density polarisation ratio (via μ), direction cosine (via k_z), quantum parameter (via H), and ion-cyclotron frequency Ω .

5 Numerical Analysis

In the previous section, we have described the dynamics of IA cnoidal waves analytically in a magnetised quantum plasma in the presence of degenerate electrons with separated spin-up and spin-down population. In the present investigation, numerically it is confirmed that the nonlinear coefficient (A) and dispersion coefficient (B) of (31) are always positive. Hence, there is the formation of only compressive (positive potential) IA cnoidal and solitary waves. However, in the previous study, Ahmad et al. [20] derived the Zarkharov-Kuznetsov equation and obtained only negative potential solitary structures. In other study, Hussain and Mahmood [21] studied the oscillatory and monotonic shock structures by varying the spin-polarisation density. We have focused our analysis to study numerically the effects of various plasma parameters and spin polarisation density on the propagation characteristics of IA cnoidal waves and also discussed the existence of solitary waves in the limiting case in the given magnetised quantum degenerate plasma. In our present work, we have mainly analysed the effects of density of spin-up and spin-down electrons through the density polarisation ratio (i.e. μ) on the maximum amplitude of cnoidal waves. For numerical analysis, the plasma parameters are chosen as $n_0 =$ $10^{26} - 10^{29} \text{cm}^{-3}$, $B_0 = 10^3 - 10^4 G$, and the temperature of the system is $10^5 K$ in the dense astrophysical plasma regions of white dwarfs [32, 33]. We have chosen H = 0.2for various plots with magnetic field intensity $B_0 = 10^4 G$, Fermi temperature $T_F = 10^5 K$, and plasma density $n_0 =$ 10^{27}cm^{-3} .

Figure 1 presents the variation of phase velocity v_{ph} with μ for different values of direction cosine (via k_z). It has been found that with increase in the value of μ , the phase velocity (v_{ph}) decreases, whereas as the value of k_z rises, there is enhancement in the value of phase velocity. It can be well explained from the expression of phase velocity given by (21). The phase velocity is directly proportional to the direction cosine k_z and inversely proportional to the density polarisation ratio, which lead to the aforementioned variation in the characteristics of phase velocity. The variation in the maximum amplitude of cnoidal waves and the depth of corresponding Sagdeev

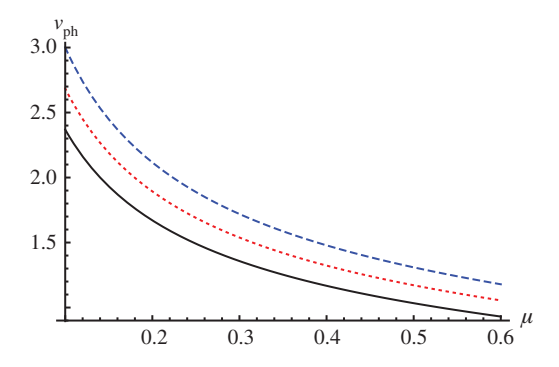
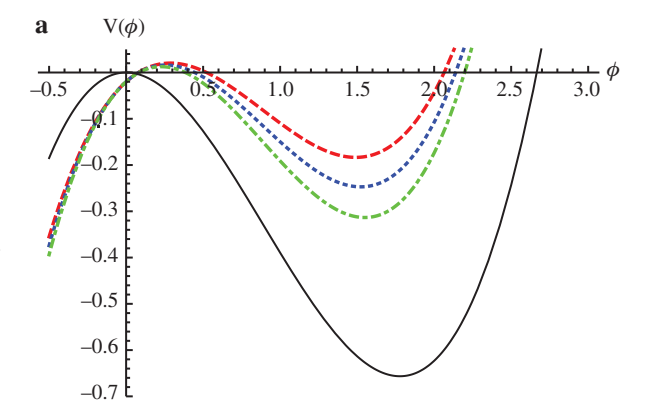


Figure 1: (Colour online) Variation of the phase velocity v_{ph} vs. μ for the different values of k_z . Solid (black) curve: $k_z = 0.75$; dotted (red) curve: $k_z = 0.85$; dashed (blue) curve: $k_z = 0.95$.

potential is analysed using (33) for different values of ioncyclotron frequency (Ω) with $\mu=0$ and is depicted in Figure 2a. Clearly, the solid (black) curve represents the Sagdeev potential corresponding to IA solitary waves with $\rho_0=0$ and $E_0=0$, whereas for finite value of $\rho_0(=0.3)$ and $E_0(=0.2)$, the other curves represent the Sagdeev



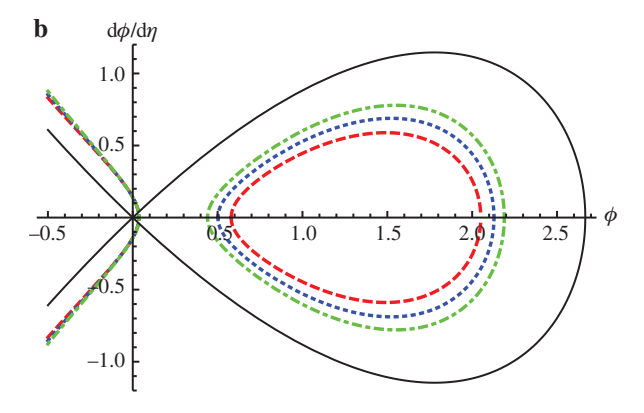
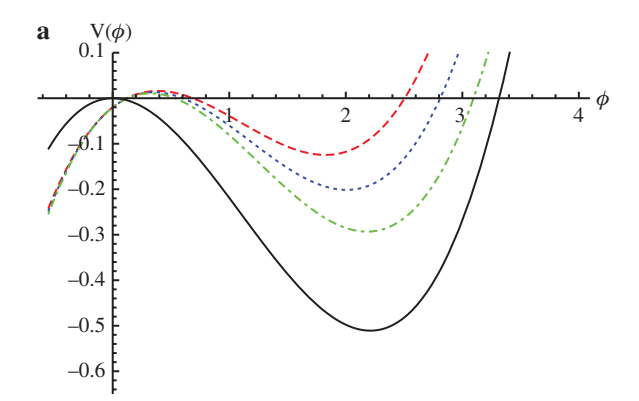


Figure 2: (Colour online) Variation of (a) Sagdeev potential of IA cnoidal waves $V(\phi)$ vs. ϕ , (b) phase plot for ion IA cnoidal waves for different values of Ω with $\mu=0$, $k_z=0.30$, H=0.2, U=0.3, $E_0=0.2$, and $\rho=0.3$. Dashed (red) curve: $\Omega=0.35$; dotted (blue) curve: $\Omega=0.37$; dot-dashed (green) curve: $\Omega=0.39$; solid (black) curve: soliton with $\Omega=0.35$, $\rho_0=0$ and $E_0=0$.

potential corresponding to the IA cnoidal waves in a quantum degenerate plasma. The roots ϕ_0 , ϕ_1 , and ϕ_2 given in (38) depict the motion of the pseudoparticle. The domain between the roots $\phi_1 < \phi < \phi_2$ confines the back-and-forth periodic oscillations of the pseudoparticle, and it cannot reach point ϕ_0 because of the potential barrier. In Figure 2a, the rise in the value of Ω enhances the maximum amplitude and depth of the Sagdeev potential $V(\phi)$. This occurs due to the fact that $V(\phi)$ is dependent on the dispersion coefficient (B), which contains the quantity ion-cyclotron frequency (Ω). The maximum amplitude of IA cnoidal wave increases as Ω (ion-cyclotron frequency) increases, and the depth of the Sagdeev potential increases along the negative axis of $V(\phi)$. As $V(\phi)$ is dependent on coefficient B (which is sensitive to any variation in Ω), any change in Ω leads to change in B, which subsequently changes $V(\phi)$. In this case, when Ω increases, B decreases [see (33)]. With the small value of B in the denominator of (33) makes $V(\phi)$ larger. Also, the Sagdeev potential $V(\phi)$ corresponding to the IA cnoidal waves does not vanish at $\phi = 0$, whereas for the IA solitary

wave $V(\phi)|_{\phi=0}=0$ (for $\rho_0=0$ and $E_0=0$). The phase plot, which shows the similar variation in the characteristics of IA cnoidal waves with the varying value of ion-cyclotron frequency (via Ω), is shown in Figure 2b. The black solid curve, called the separatrix, represents the characteristics of IA solitary waves, whereas all other curves lying inside the separatrix are characterised as the IA cnoidal waves. The pseudoparticle for IA cnoidal wave oscillates between the two real zeros of the Sagdeev potential, ϕ_1 and ϕ_2 , as clearly depicted in Figure 2a. This means that potential structure is reappearing, and the distance between recurrences of wave shapes corresponds to one wavelength. Also, in Figure 3a, Sagdeev potential $V(\phi)$ is plotted against ϕ for $\mu = 1$ for different values of ion-cyclotron frequency Ω . From Figure 3, we have depicted that with the increase in value of Ω , there is also enhancement in both maximum amplitude of cnoidal waves and depth of the Sagdeev potential. On comparing both Figures 2 and 3, it is observed that the maximum amplitude of cnoidal waves for zero spin polarisation case $\mu = 0$ is smaller than the maximum amplitude of cnoidal waves for strongly spin-polarised case $\mu = 1$.



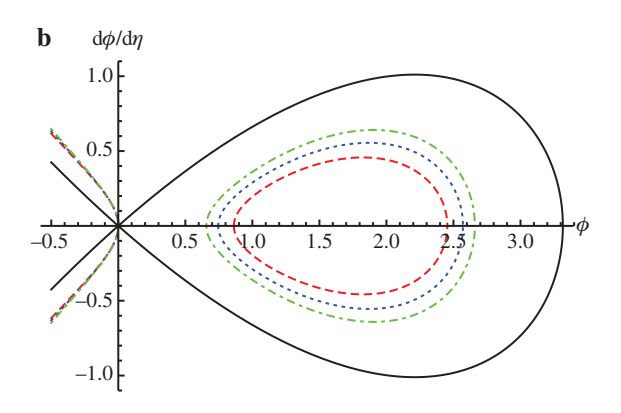
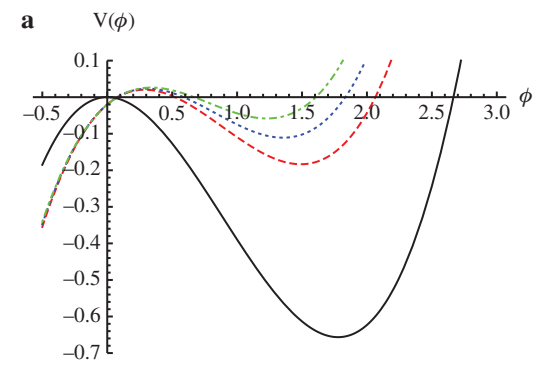


Figure 3: (Colour online) Variation of (a) Sagdeev potential of IA cnoidal waves $V(\phi)$ vs. ϕ , (b) phase plot for ion IA cnoidal waves for different values of Ω with $\mu=1$, $k_z=0.30$, H=0.2, U=0.3, and $\rho=0.2$. Dashed (red) curve: $\Omega=0.35$; dotted (blue) curve: $\Omega=0.37$; dot-dashed (green) curve: $\Omega=0.39$; solid (black) curve: soliton with $\Omega=0.35$, $\rho_0=0$, and $E_0=0$.



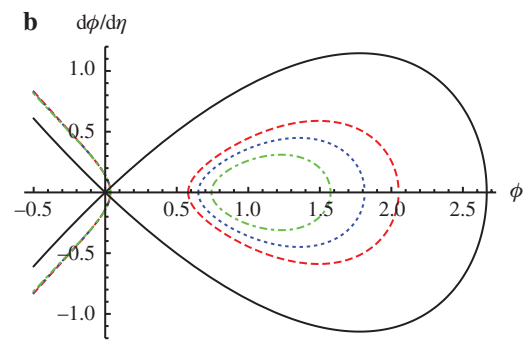
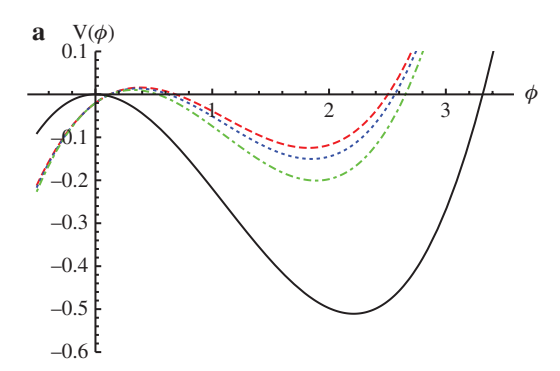


Figure 4: (Colour online) Variation of (a) Sagdeev potential of IA cnoidal waves $V(\phi)$ vs. ϕ , (b) phase plot for ion IA cnoidal waves for different values of direction cosine k_z with $\mu=0$, $\Omega=0.35$, U=0.3, H=0.2, $E_0=0.2$, and P=0.3. Dashed (red) curve: $E_0=0.30$; dotted (blue) curve: $E_0=0.32$; dot-dashed (green) curve: $E_0=0.34$; solid (black) curve: soliton with $E_0=0.34$; and $E_0=0.34$; solid (black) curve: soliton with $E_0=0.34$; and $E_0=0.34$; solid (black) curve: soliton with $E_0=0.34$; soli

The influence of the varying value of the parameter k_z (i.e. direction cosine) on the characteristics of Sagdeev potential and phase plane plot is depicted in Figure 4. With the increase in the value of k_z , both the maximum amplitude and depth of the Sagdeev potential are reduced as shown in Figure 4a. The phase plane plot for the different values of k_z is shown in Figure 4b. It is clearly visible from both figures that for $\rho_0 \neq 0$ and $E_0 \neq 0$, the phase curves show the repetitive behaviour on the same path. The pseudoparticle gets reflected back due to the potential force and starts oscillating between the two points whenever $dV(\phi)/d\eta = 0$ (i.e. when the pseudoparticle velocity becomes zero) as $dV(\phi)/d\phi$ does not get vanished. In physical space, one wavelength is equivalent to one cycle of the phase plot completed by the pseudoparticle. Hence, as the value of direction cosine k_z rises, there is fall in the wavelength of IA cnoidal waves as depicted in Figure 4b. Figure 5a depicts the variation of Sagdeev potential for the different values of k_z for $\mu = 1$. Here, with the increase in value of k_z , the maximum amplitude and depth of the Sagdeev potential of IA cnoidal wave are decreased. But again, on comparing both Figures 4 and 5, there is significant variation in the maximum amplitude



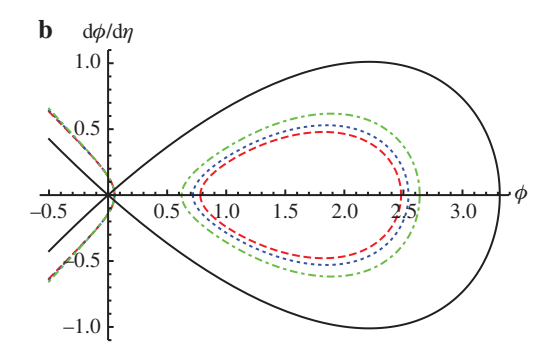


Figure 5: (Colour online) Variation of (a) Sagdeev potential of IA cnoidal wave $V(\phi)$ vs. ϕ (b), phase plot for ion IA cnoidal waves for different values of direction cosine k_z with $\mu=1$, $\Omega=0.35$, U=0.3, H=0.2, $E_0=0.2$, and $\rho=0.2$. Dashed (red) curve: $k_z=0.30$; dotted (blue) curve: $E_z=0.32$; dot-dashed (green) curve: $E_z=0.34$; solid (black) curve: soliton with $E_z=0.34$; and $E_z=0.34$; and $E_z=0.34$; solid (black) curve: soliton with $E_z=0.34$; and $E_z=0.34$; solid (black) curve: soliton with $E_z=0.34$; and $E_z=0.34$; solid (black) curve: soliton with $E_z=0.34$; and $E_z=0.34$; solid (black) curve: soliton with $E_z=0.34$; and $E_z=0.34$; solid (black) curve: soliton with $E_z=0.34$; and $E_z=0.34$; solid (black) curve: soliton with $E_z=0.34$; and $E_z=0.34$; solid (black) curve: soliton with $E_z=0.34$; solid (black) curve: soliton with $E_z=0.34$; and $E_z=0.34$; solid (black) curve: soliton with $E_z=0.34$; and $E_z=0.34$; solid (black) curve: soliton with $E_z=0.34$; solid (black) c

of Sagdeev potential of IA cnoidal wave. The maximum amplitude of Sagdeev potential of IA cnoidal wave for zero spin polarisation ratio $\mu=0$ is smaller than the case for spin polarisation ratio $\mu=1$.

Figure 6a and b illustrate the variation of pulse profile of positive potential IA cnoidal waves for different values of ion-cyclotron frequency (via Ω) for $\mu = 0$ and $\mu = 1$, respectively. The maximum amplitude of IA cnoidal waves increases with the increasing value of Ω . It can be seen that the amplitude for $\mu = 1$ is larger as compared to the amplitude of pulse profile for $\mu = 0$. In the limiting case (for $\rho_0 = 0$ and $E_0 = 0$), we have also depicted the pulse profile of IA solitary waves in both figures. This can be verified from the fact that (33) is dependent on dispersion coefficient B, which is sensitive to ion-cyclotron frequency Ω , and any change in Ω causes a variation in dispersion coefficient B, which leads to the change in the maximum amplitude of IA cnoidal wave profile. The solid (black) curve represents the wave profile of IA solitary waves, which does not repeat itself like IA cnoidal waves and hence represents the characteristics of IA solitary waves. It is remarked that density spin polarisation has a significant influence on the propagation characteristics of cnoidal as well as solitary waves.

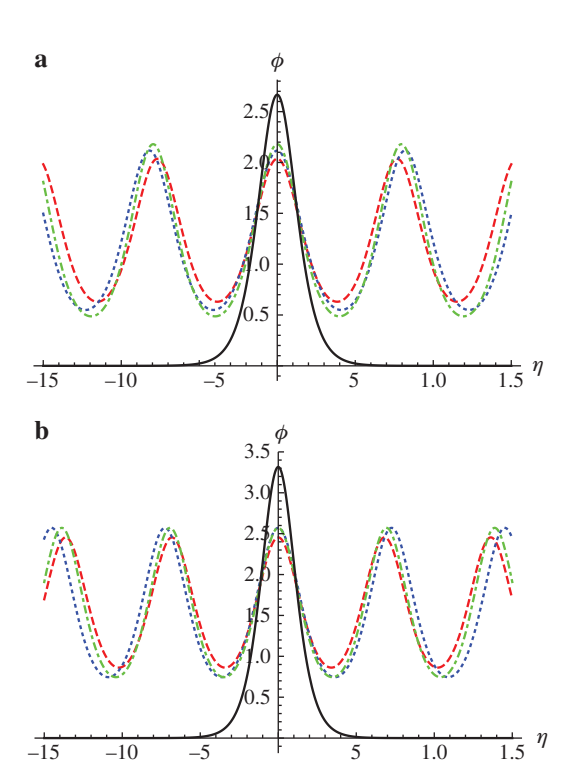


Figure 6: (Colour online) Variation of pulse profile of IA cnoidal wave (a) $\mu=0$, (b) $\mu=1$ for different values of Ω with U=0.3, H=0.2, $E_0=0.2$, and $\rho_0=0.3$. Dashed (red) curve: $\Omega=0.35$; dotted (blue) curve: $\Omega=0.37$; dot-dashed (green) curve: $\Omega=0.39$; solid (black) curve: soliton with $\Omega=0.35$, $\rho_0=0$, and $E_0=0$.

6 Conclusions

The propagation characteristics of IA cnoidal waves are studied in the presence of magnetic field considering degenerate electrons with spin-up and spin-down states in quantum plasmas. We have considered that the Fermi step of the spin-up electrons is shorter than the Fermi step of the spin-down electrons, and due to this fact, there is no contribution of the outer-species collisions. Also, we are considering spin-up and spin-down electrons as different species, and their direction is related to a preferable direction in space for uniform external magnetic field, which lies along the *z*-direction in the present case. The equations of state for the spin-up and spin-down electrons are different due to the presence of external magnetic field, which changes an equilibrium concentration of each species. For nonlinear analysis, we have derived KdV equation by using the reductive perturbation method. Only positive potential (compressive) IA cnoidal waves and in the limiting case solitary waves are observed in the given plasma system. The influence of density spin polarisation via μ [for strongly spin-polarised ($\mu = 1$), zero spin-polarisation density ($\mu = 0$)] and other plasma parameters such as ion-cyclotron frequency (via Ω), quantum parameter (via H), and direction cosine (via k_z) has been analysed numerically on the dynamics of compressive cnoidal waves. The phase velocity for IA cnoidal waves rises with the increment in the value of k_z . The maximum amplitude of IA cnoidal waves and depth of the Sagdeev potential are enhanced (reduced) with the rising value of Ω (k_z) . On comparing the variation of Sagdeev potential with the different values of Ω and k_z for both cases of spin polarisation (i.e. for $\mu = 0$ and $\mu = 1$), we have concluded that there is growth in the maximum amplitude of IA cnoidal waves as the value of μ changes from $\mu = 0$ to $\mu = 1$. It is emphasised that spin polarisation plays a very vital role for the variation in the characteristics of IA cnoidal waves. The findings of the present investigation may have paramount importance in different environments of dense astrophysical plasma regions, specifically like neutron stars, white dwarfs, and so on.

Acknowledgement: The authors are thankful to the reviewers for their critical and positive comments. R.K. acknowledges DST, Government of India, under DST-Purse scheme for financial support. This work is also supported by DRS-II (SAP) No. F/530/17/DRS-II/2015 (SAP-1) University Grants Commission, New Delhi, India.

References

- [1] F. Calvayrac, P. G. Reinhand, E. Suraud, and C. Ullrich, Phys. Rep. 337, 493 (2000).
- [2] L. Stenflo, P. K. Shukla, and M. Marklund, Europhys. Lett. 74, 844 (2006).
- [3] Y. I. Salamin, S. X. Hu, Z. Hatsagortsyam, and C. H. Keital, Phys. Rep. 427, 41 (2006).
- [4] A. K. Harding and D. Lai, Rep. Prog. Phys. 69, 2631 (2006).
- [5] S. Chandrashekhar, Astrophys. J. 74, 81 (1931).
- [6] S. Chandrashekhar, Philos. Mag. 11, 592 (1931).
- [7] S. Chandrashekhar, Mon. Not. R. Astron. Soc. 170, 405 (1935).
- [8] P. K. Shukla and B. Eliasson, Rev. Mod. Phys. 83, 885 (2011).
- [9] D. Bohm, Phys. Rev. 85, 166 (1952).
- [10] F. Haas, L. G. Garcia, J. Goedert, and G. Manfredi, Phys. Plasmas 10, 3858 (2003).
- [11] F. Haas, Phys. Plasmas 12, 062117 (2005).
- [12] P. K. Shukla, B. Eliasson, and L. Stenflo, Phys. Plasmas 19, 072302 (2002).
- [13] G. Charbrier, F. Douchin, and A. Y. Potekhin, J. Phys. Condens. Matter 14, 9133 (2002).
- [14] M. Marklund and G. Brodin, Phys. Rev. Lett. 98, 025001 (2007).
- [15] G. Brodin and M. Marklund, New J. Phys. 9, 277 (2007).
- [16] A. Mushtag and S. V. Vladimirov, Phys. Plasmas 17, 102310
- [17] P. A. Andreev, Phys. Rev. E 91, 033111 (2015).
- [18] Z. Iqbal and P. A. Andreev, Phys. Plasmas 23, 062320 (2016).
- [19] B. M. Askerov and S. R. Figarova, Thermodynamics, Gibbs Method and Statistical Physics of Electron Gases, Springer-Verlag, Berlin 2010.
- [20] R. Ahmad, N. Gul, M. Adnan, and F. Y. Khattak, Phys. Plasmas 23, 112112 (2016).
- [21] S. Hussain and S. Mahmood, Phys. Plasmas 24, 102106 (2017).
- [22] K. Konno, T. Mitsuhashi, and Y. H. Ichikawa, J. Phys. Soc. Jpn. 46, 1907 (1979).
- [23] A. V. Gurevich and L. Stenflo, Phys. Scripta 38, 855 (1988).
- [24] U. Kauschke and H. Schluter, Plasma Phys. Contr. F. 33, 1309 (1991).
- [25] E. F. El-Shamy, Phys. Rev. E 91, 033105 (2015).
- [26] H. Ur-Rehman, S. Mahmood, and S. Hussain, Phys. Plasmas **24.** 012106 (2017).
- [27] N. Kaur, M. Singh, R. Kohli, and N. S. Saini, IEEE T. Plasma Sci. **46**, 768 (2018).
- [28] N. Kaur, M. Singh, and N. S. Saini, Phys. Plasmas 25, 043704 (2018).
- [29] T. Kaladze, S. Mahmood and H. Ur-Rehman, Phys. Scripta 86, 035506 (2012).
- [30] T. Kaladze and S. Mahmood, Phys. Plasmas 21, 032306 (2016).
- [31] M. Abramowitz and I. A. Stegun, Handbook of Mathematical Function, Dover, New York 1972.
- [32] D. Koester and G. Chanmugam, Rep. Prog. Phys. 53, 837 (1990).
- [33] G. Chabrier, D. Saumon, and A. Y. Potekhin, J. Phys. A Math. Gen. 39, 4411 (2006).